

Modelling the stellar soft-photon energy density profile of globular clusters

P L Prinsloo¹, C Venter¹, I Buesching¹ and A Kopp^{1,2}

¹ Centre for Space Research, North-West University, Potchefstroom Campus, Private Bag X6001, Potchefstroom 2520, South Africa

² Institut für Experimentelle und Angewandte Physik, Christian-Albrechts-Universität zu Kiel, Leibnizstrasse 11, 24118 Kiel, Germany

E-mail: 21696764@nwu.ac.za

Abstract. Recent observations by e.g. *Fermi* Large Area Telescope (LAT) and the High Energy Stereoscopic System (H.E.S.S.) have revealed globular clusters (GC) to be sources of high-energy (HE) and very-high-energy (VHE) γ -rays. It has been suggested that the presence of large numbers of millisecond pulsars (MSPs) within these clusters may be either directly responsible for these γ -ray fluxes through emission of pulsed curvature radiation, or indirectly through the injection of relativistic leptons into the cluster. These relativistic particles are plausibly re-accelerated in shocks, created by the collision of stellar winds, before interacting with the soft-photon radiation field set up by the stellar population of the host cluster. Inverse Compton (IC) scattering then produces γ -radiation in the TeV band. In order to calculate the IC spectrum, an accurate profile for the energy density of the soft-photon field is required. We construct such a profile by deriving a radially-dependent expression for the stellar energy density, and then solve it numerically. As a next step, the average energy density values for three different regions of the cluster (demarcated by its core, half-mass, and tidal radii) are determined, which we consequently import into an existing radiation code to predict the TeV γ -ray spectrum. As an application, we consider the case of Terzan 5, boasting a population of 34 radio MSPs, and compare our predicted spectrum with that recently measured by H.E.S.S. We lastly comment on the accuracy of our model and discuss possible improvements.

1. Introduction

Globular clusters (GC) are large spherical collections of roughly a hundred thousand to a million gravitationally bound stars [1]. The cluster cores contain the more massive stars and have very high stellar densities, which creates favourable conditions for binary interaction [2]. Expressions for the mass density profile of a GC can be constructed using Michie-King multi-mass models, for example [3]

$$\rho(r) = \rho_0 \begin{cases} 1 & r < r_c \\ (r_c/r)^2 & r_c < r < r_h \\ (r_c r_h)^2 / r^4 & r_h < r < r_t. \end{cases} \quad (1)$$

It would appear as if GCs are suitable to host large populations of millisecond pulsars (MSPs), since GCs are found to harbour a great number of stellar binary members [4, 5], and since they are ancient objects with mean ages of 12.8 ± 1.0 Gyr [6] at which one would expect to find many

stellar remnants. In fact, the presence of 143 pulsars in 27 different clusters has been established to date¹, although it has been predicted that there may be as many as a few hundred MSPs in cluster centres [7].

Recent observations have revealed several GCs to be sources of HE and VHE² γ -radiation. The Large Area Telescope (LAT) aboard the *Fermi* Gamma-ray Space Telescope, for instance, detected these highly energetic γ -ray emissions from clusters such as 47 Tucanae and Terzan 5 (Ter5) [9–12]. Ter5 was also revealed by the ground-based High Energy Stereoscopic System (H.E.S.S.) as a source of VHE γ -radiation [13], and since GCs are known hosts of MSPs, these ancient stars are thought to be responsible for the γ -ray fluxes. Ter5, in particular, hosts the largest known number of radio MSPs of all GCs with a population of 34¹, and also boasts one of the highest central densities and stellar collision rates [14]. It is situated at a distance of 5.9 ± 0.5 kpc from Earth [15], has core, half-mass and tidal radii of 0.15', 0.52' and 4.6' respectively, a total luminosity of $8 \times 10^5 L_\odot$ [14], and is expected to harbour as many as 200 MSPs [11, 16].

One particular manner in which the energy of pulsars dissipates is through the ejection of particles in the form of relativistic pulsar winds [17], where they are modelled to accelerate to relativistic speeds either in the magnetosphere of the MSP [18] or due to relativistic shocks caused by the collision of pulsar winds [19]. Though this is expected to account for a very small fraction of a pulsar's spin-down luminosity, with an energy conversion efficiency of as little as $\eta \sim 0.01$ [20], it is still considered to be responsible for emission in the TeV band [8] and thus able to account for these emissions detected from GCs. The radiation mechanism thought to be responsible³ is inverse Compton (IC) scattering where relativistic leptons up-scatters soft (or low-energy) photons to γ -rays. The IC-emissivity, related to the scattered photon spectrum per incident electron, is [22],

$$Q_{\text{comp},j}(E_\gamma, t) = 4\pi \int_0^\infty n_j(\epsilon, r) d\epsilon \times \int_{E_e, \text{thresh}}^{E_e, \text{max}} J_e(E_e, t) F(\epsilon, E_\gamma, E_e). \quad (2)$$

Here the J_e component is a steady-state particle spectrum related to the lepton injection spectrum, which is in turn related to the pulsar spin-down luminosity, and also entails the particle transport. The F component in equation (2) relates to the cross-section of the interaction. See [22, 23] for more detail. What is of interest for the purposes of this paper is the n_j component, which is a photon number density with subscript j corresponding to one of three soft photon components (cosmic microwave background (CMB), infrared (IR) or starlight). For a blackbody it is given as follows [22],

$$n_j(\epsilon) = \frac{15U_j}{(\pi k T_j)^4} \frac{\epsilon^2}{e^{(\epsilon/kT_j)} - 1}. \quad (3)$$

Here ϵ represents the initial energy of the photon before scattering, k is the Boltzmann constant, and T_j and U_j represent the temperature and energy density corresponding to each soft photon component. In an environment such as that created by GCs, one would expect the vast stellar populations to induce a prominent starlight component with high energy density U , which decreases, like the stellar population density, with increasing distance from the cluster centre.

In some models, the energy density has been represented as average values within two zones, demarcated by the cluster centre, the core and half-mass radii [18, 20]. It is the objective of this paper to construct a radially-dependent expression for the stellar soft-photon energy density of a GC (see Section 2), and to solve it numerically for the case of Ter5 (see Section 3). We then use this profile to predict the γ -radiation spectrum of MSPs within Ter5 (see Section 3) whilst

¹ see <http://www2.naic.edu/~pfreire/GCpsr.html>, doa: 30 June 2012

² HE: High-energy $E > 100$ MeV, VHE: Very-high-energy $E > 100$ GeV [8]

³ For an alternative interpretation, see [21]

regarding IC scattering as the predominant radiation mechanism. Following this, conclusions can be made regarding the significance of the result, comparisons can be made with the resulting spectra of other models, and the accuracy of the model can be assessed (see Section 3-4).

2. Constructing the energy density profile

To initiate the construction of the radially-dependent energy density profile, it was assumed that the stars in a GC radiate like blackbodies. By integrating the blackbody radiation intensity, that is $I_\nu = (2h\nu^3/c^2)(\exp(h\nu/kT) - 1)^{-1}$ [24] with units $\text{erg} (\text{s cm}^2 \text{ Hz sr})^{-1}$, over all frequencies, the total intensity in terms of temperature was obtained. Then, by introducing the radiation density constant $a = 4\sigma/c$ [1] and by scaling the result to compensate for the distance to the star (d) and its total radiating surface area ($\propto R^2$), a result giving the total energy radiated by a single star per unit volume, $u_s = (4\pi/c)(R^2/d^2)I$, was obtained. Assuming that stars in GCs are distributed spherically symmetrical with the cluster centre as origin, replacing d with the separation distance $|\mathbf{r} - \mathbf{r}'|$ between the contributing source at radius r' and an observer within the cluster at r , and assuming identical properties for all the stars, the preceding result was expanded to include the energy density contributions of all the stars in the cluster. Rewriting the integral constructed to obtain the total energy density of the amount of stars per radial interval $N(r)dr$ as a volume integral of mass-density (divided by the average stellar mass; $\rho/\bar{m} dV$) allowed the expanded result to be expressed as a triple integral. The result was a radially-dependent expression for the starlight energy density of GCs, given by

$$u(r) = \frac{8\pi^2 R^2}{c} \frac{I}{\bar{m}} \frac{1}{r} \int_0^{r_t} \rho(r') r' \ln \left(\frac{|r' + r|}{|r' - r|} \right) dr', \quad (4)$$

where R is the stellar radius, \bar{m} is the average stellar mass and c is the speed of light. The mass-density $\rho(r')$, given by equation (1), was normalised by setting the total cluster mass $M_{\text{total}} = N_{\text{total}}\bar{m} = \int \rho(r)dV = 4\pi \int \rho(r)r^2 dr$, where N_{tot} is the total number of stars in the cluster and is obtained from L_{tot}/L_\odot . Here L_{tot} is the total luminosity of the cluster, L_\odot is the solar luminosity and all stars are assumed to have solar luminosities as a first approximation. The central mass-density ρ_0 in equation (1) could then be expressed in terms of measurable cluster parameters and the integral in equation (4) solved numerically.

3. Results and discussion

A general proportionality relation of $u \propto N_{\text{tot}} R^2 T^4$ can be deduced for the energy density from equation (4). This effectively means that doubling either the total number of stars, the stellar radius, or the stellar temperature will result in an energy density increase of factor 2, 4 or 16 respectively. Notice that the energy-density, according to this model, shows no dependence on the mean stellar mass. This is because the central mass-density ρ_0 , which was determined by normalising equation (1), contains a factor \bar{m} which cancels with that contained in the denominator of equation (4). Furthermore, solving equation (4) numerically, using the measured parameters for Ter5 and assuming solar properties for its stars, an energy density profile is obtained as shown by the solid black curve in Figure 1. This energy density profile is then divided into three discrete zones, as shown in Figure 1. The average energy densities for each of these three zones are obtained as 11×10^3 , 6.3×10^3 and 170 eV cm^{-3} , which are consequently imported into existing radiation code [18] to calculate the corresponding IC spectrum. The temperature and energy density of the CMB are chosen as 2.76 K and 0.27 eV cm^{-3} , and the cluster magnetic field strength as $1 \mu\text{G}$. A number of 8×10^5 stars is deduced from the total cluster luminosity, while the distance and cluster radii are taken as mentioned in Section 1. Regarding the injection spectrum, a power law is assumed and the minimum and maximum particle energies taken as 0.1 GeV and 100 TeV respectively, with a spectral index of 1.6.

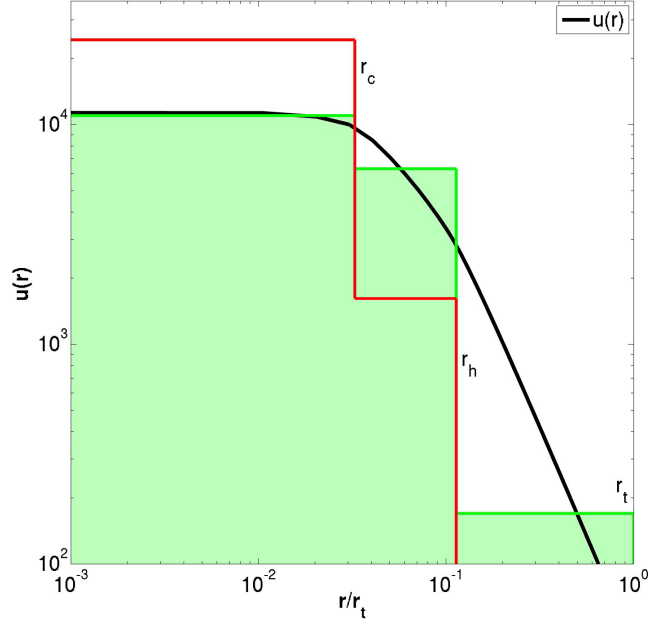


Figure 1. Comparison of energy densities calculated for Ter5. The average energy densities for three regions (shown in green), demarcated by the core, half-mass and tidal radii, are calculated from the energy-density profile (solid black line) of Ter5. Shown in red are the average energy densities for two zones used by [18, 20].

Furthermore, the number of MSPs is taken as 100, the average spin-down luminosity $\langle \dot{E} \rangle$ as $2 \times 10^{34} \text{ erg s}^{-1}$ and the particle energy conversion efficiency η as 1%. Having imported all of these parameters, we obtain Figure 2.

The resultant spectrum obtained from the contribution from only two zones is indicated with a faint blue line (see Figure 2), and does not differ much from the result by [20] (shown in dark green). The small difference stems from a difference in the average energy density values used. However, with the inclusion of the third zone (of which the contribution is shown with the top faint red line), the resultant spectrum (thick, solid blue line) is shaped in such a way that it can be well aligned to fit the H.E.S.S. data. For the best alignment however, it is necessary to scale the spectrum up by a factor 3, which means that if the IC-spectra depends roughly on $N_{\text{tot}} \times N_{\text{MSP}} \times \eta_p \times \langle \dot{E}_{\text{rot}} \rangle$, then the total number of stars and MSPs, the energy conversion efficiency and the spin-down luminosity must each be scaled in such a manner that a resultant increase of factor 3 occurs.

We have estimated the systematic error on the energy density profile using ‘bootstrapping’ and involving several sets of possible model parameters. This was done by randomly generating up to a thousand stellar masses from 1 to $2 M_{\odot}$, and calculating each mass’ corresponding stellar radius and temperature by using upper main sequence relations. Then, for every set of parameters, the energy density at each incremental distance from the cluster centre was calculated using equation (4). From there the average energy density \bar{u} and standard error σ were calculated at each of these radii. The upper and lower 1σ error margins are consequently estimated at $2\bar{u}$ and $0.1\bar{u}$, respectively. Furthermore, it is worth noting that these error margins are propagated to the IC spectrum in a linear fashion. The error estimates for the energy density profile may be conservative, seeing as though the stars occurring within GCs may not follow upper main sequence relations as was assumed above. It can be remarked, however, that stars occurring within GCs are considered to be old stars that have expelled most of their mass [1],

and therefore limiting stars to masses smaller than $2 M_{\odot}$, as was done above, may indeed be justified.

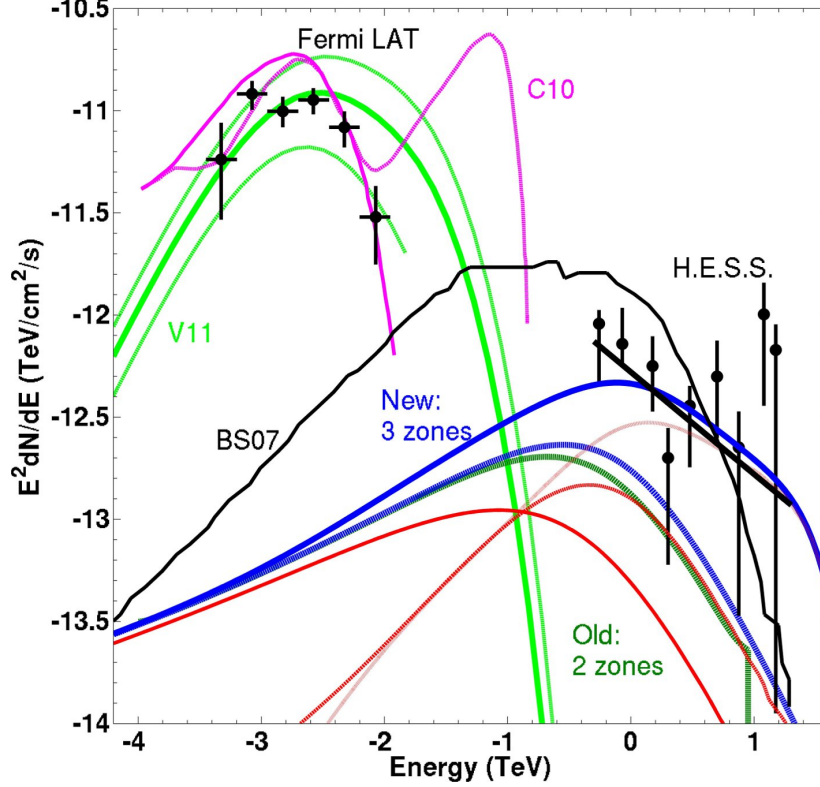


Figure 2. Predicted γ -ray spectra for Ter5. Here, the contributions to the IC spectrum of the energy densities for the three zones constructed in this paper are shown in red, and their collective contribution with a solid, bright blue line. The faint blue line shows the collective contribution of the first two zones constructed in this paper. Take note that these spectra have been scaled up with a factor of three so that the resultant spectrum is better aligned with the H.E.S.S. data. Furthermore, the IC spectrum obtained by [20] is shown in dark green and is labelled ‘Old: 2 Zones’, while a scaled prediction of [19] is shown in black with label ‘BS07’. The lime green and magenta lines (labelled V11 and C10) are the spectra calculated for the HE band [25, 26].

4. Conclusions

It has been argued that GCs, having a high number of stars in late evolutionary stages and a high binary encounter rate, are suitable to host large populations of MSPs. In addition, GCs have been revealed by *Fermi* LAT and H.E.S.S. as sources of HE and VHE γ -radiation. Such γ -ray emissions have been modelled to arise from the IC scattering of stellar soft photons due to interactions with relativistic particles injected by MSPs. As part of the calculation of the IC spectrum, it was necessary to construct a radially-dependent expression for the soft photon energy density of GCs. We derived this expression analytically, normalised it, and then solved it numerically for the parameters of the GC Ter5. Having divided the profile for Ter5 into three zones (while awaiting more refined particle transport calculations which would allow us to use a greater number of zones), we calculated an average energy density for each zone and consequently used these values to predict the IC spectrum of Ter5. The resultant spectrum was

compared to that generated by earlier models as well as to H.E.S.S. data. We found that the predicted spectrum provides a good fit to the H.E.S.S. data if scaled up by a factor 3. This factor may be obtained by, for example, scaling N_{tot} , N_{MSP} , η_p and $\langle \dot{E}_{\text{rot}} \rangle$ each by roughly 1.3. It can be concluded that the addition of the third zone greatly improved the model's performance when comparing our IC spectrum with those of models that included fewer zones. We note that the H.E.S.S. data are nearly included within the error margins of the predicted IC spectrum (even without scaling the data).

This paper can be expanded in a number of ways. When calculating the error estimates on the energy density profile, Hertzsprung-Russel diagrams may be consulted to find an upper limit to the mass we might expect stars in GCs to have. Also, by investigating and using the correct relations between stellar properties for the stellar populations present in GCs, a higher accuracy may be achieved on the energy density profile. The energy density can be derived again for asymmetrically distributed sources, and the soft photon contribution of the Galactic background should be taken into account [26]. In addition, the surface brightness profile implied by equation (1) should be compared to the observed optical surface brightness to assess the validity of equation (1). Furthermore, possible ways of improving the IC calculation include constructing a cluster magnetic field profile and using refined transport equations for a better modelling of the time-evolution of the particle injection spectrum. The latter will allow the average energy densities of a greater number of zones to be imported into the radiation code without loss of stability. This might further strengthen the correlation of the predicted IC spectrum with observational data.

Acknowledgements

This research is based upon work supported by the South African National Research Foundation.

References

- [1] Tayler R J 1994 *The Stars: Their Structure and Evolution* (Cambridge University Press)
- [2] Pooley D and Hut P 2006 *IAU Joint Discussion* vol 14
- [3] Kuranov A G and Postnov K A 2006 *Astronomy Letters* **32** 393–405
- [4] Alpar M A, Cheng A F, Ruderman M A and Shaham J 1982 *Nature* **300** 728–730
- [5] Camilo F and Rasio F A 2005 *Binary Radio Pulsars* (*Astron. Soc. of the Pac. Conf. Series* vol 328) ed Rasio F A and Stairs I H p 147
- [6] Krauss L M 2000 *Physics Reports* **333** 33–45
- [7] Tavani M 1993 *Astrophys. J* **407** 135–141
- [8] Bednarek W 2011 *High-Energy Emission from Pulsars and their Systems* ed Torres D F and Rea N p 185
- [9] Abdo A A *et al.* 2009 *Science* **326** 1512
- [10] Abdo A A *et al.* 2010 *Astron. Astrophys.* **524** A75
- [11] Kong A K H, Hui C Y and Cheng K S 2010 *Astrophys. J* **712** L36–L39
- [12] Tam P H T, Kong A K H, Hui C Y, Cheng K S, Li C and Lu T N 2011 *Astrophys. J* **729** 90
- [13] Abramowski A *et al.* 2011 *Astron. Astrophys.* **531** L18
- [14] Lanzoni B *et al.* 2010 *Astrophys. J* **717** 653–657
- [15] Ferraro F R *et al.* 2009 *Nature* **462** 483–486
- [16] Fruchter A S and Goss W M 2000 *Astrophys. J* **536** 865–874
- [17] Reynolds S P and Chevalier R A 1984 *Astrophys. J* **278** 630–648
- [18] Venter C, De Jager O C and Clapson A C 2009 *Astrophys. J* **696** L52
- [19] Bednarek W and Sitarek J 2007 *Mon. Not. R. Astron. Soc.* **377** 920–930
- [20] Venter C and de Jager O C 2008 *AIP Conf. Ser.* vol 1085 ed Aharonian F A *et al.* pp 277–280
- [21] Venter C, Buesching I, Kopp A, Clapson A C and de Jager O C 2012 *These proceedings*
- [22] Zhang L, Chen S B and Fang J 2008 **676** 1210–1217
- [23] Blumenthal G R and Gould R J 1970 *Reviews of Modern Physics* **42** 237–271
- [24] Oetken L 1988 *Astronomische Nachrichten* **309** 322–322
- [25] Venter C, de Jager O C, Kopp A and Büsching I 2011 *ArXiv e-prints* (Preprint [arXiv:1111.1289](https://arxiv.org/abs/1111.1289))
- [26] Cheng K S, Chernyshov D O, Dogiel V A, Hui C Y and Kong A K H 2010 *Astrophys. J* **723** 1219–1230